

Three-Dimensional Structure of the Regularly Constructed Surface Layer from *Synechocystis* sp. Strain CLII

BENGT KARLSSON,¹ TIMO VAARA,² KARI LOUNATMAA,^{3*} AND HELGE GYLLENBERG²

Department of Structural Chemistry, Arrhenius Laboratory, University of Stockholm, Stockholm, Sweden,¹ and Departments of Microbiology² and Electron Microscopy,³ University of Helsinki, Helsinki, Finland

Received 3 March 1983/Accepted 26 September 1983

The isolated, outermost cell wall layer from *Synechocystis* sp. strain CLII is described using electron microscopy and Fourier reconstruction to study the three-dimensional structure of the proteins within the layer to a resolution of ca. 3 nm. This surface layer forms regular hexagonal arrays ($a = b = 15.2$ nm). The two-dimensional space group is p6. The monomer proteins form hexamers arranged around a central hollow cylinder. The linkers between the hexamers are of the delta type and are located approximately in the central section between the top and bottom of the protein layer.

Many kinds of bacteria are known to bear in their cell surfaces regularly structured surface layers which are often composed of hexagonally or tetragonally arranged protein or glycoprotein subunits (3, 24, 25). These layers are usually called S-layers or external layers. We will use the term S-layer throughout this paper, in accordance with the now conventionally adopted nomenclature. The regularly constructed S-layers of *Aquaspirillum serpens* (8, 9, 10, 12, 18, 30), *Spirillum putridiconchylum* (4, 5, 6, 31), and *Sporosarcina ureae* (1, 29) are particularly well characterized. Regularly constructed S-layers have been described also on numerous other bacteria of various types and from various environments (24), e.g., *Sulfolobus acidocaldarius* (37), *Bacillus sphaericus* (13), *Caulobacter crescentus* (26), *Halobacterium* species (7), *Micrococcus radiodurans* (19), and *Aeromonas salmonicida* (16, 33). The regularly constructed S-layers have been thought to have protective function (2, 3, 33).

S-layers have also been found on some cyanobacteria, a diversified group of oxygenic photosynthetic procaryotes (28), formerly called blue-green algae. They were first found by Kessel (17) on four *Microcystis* species. We described a regularly structured surface layer on *Synechocystis* sp. strain CB3 (21, 35), as well as, in a recent study on the occurrence of outermost surface structures in chroococcacean cyanobacteria (34), on 3 out of 7 *Synechocystis* strains, 1 out of 12 *Synechococcus* strains, and 1 *Microcystis* strain.

The structural knowledge about outer cell envelopes is usually limited to two-dimensional filtered projections; the filtering procedures

used include both Fourier methods and correlation averaging (23). Three-dimensional structures are to our knowledge only known in two cases: the structure of the S-layer of *Sulfolobus acidocaldarius* (32) and the outer envelope of *Clamidia trachomatis* (11). Although both these layers have hexagonal packing, their structures are quite different compared with what we report here.

MATERIALS AND METHODS

Bacterial strain and growth condition. *Synechocystis* sp. strain CLII was isolated from pasture silt near the campus of the Department of Microbiology, University of Helsinki (36) and is presently maintained in the Cyanobacterial Culture Collection of the Department of Microbiology, University of Helsinki.

The strain was grown in 10 5-liter conical flasks containing 1,000 ml of medium BG11 (27). The cultivation took place without shaking at 26°C under continuous illumination of ca. 500 lx provided by cool white fluorescent tubes (Airam, Helsinki, Finland). Under these growth conditions, the strain reached the stationary phase of growth within 3 weeks.

Isolation of cell envelope material. After growth for 2 weeks, the cells (wet weight ca. 6 g) were harvested by continuous centrifugation (ca. $5,000 \times g$ at room temperature) and suspended in 50 mM phosphate buffer (pH 8.0) supplemented with 5 mM $MgCl_2$ (PM buffer). The cell suspension was subjected to brief sonication followed by centrifugation at $1,500 \times g$ for 10 min to remove the partially "stripped" cells. The supernatant contained mainly cell envelope material, i.e., the S-layer associated with the outer membrane. This material was collected by centrifugation at $20,000 \times g$ for 30 min, washed with PM buffer, and finally lyophilized.

Electron microscopy. (i) Thin sections. For the thin sections, cells of *Synechocystis* sp. strain CLII were stained with ruthenium red (BDH, Poole, England) by the method of Luft (22), with 1,500 ppm of strain

added to the fixative. The fixative was 3% glutaraldehyde (Leiras, Turku, Finland) in 0.1 M sodium phosphate buffer (pH 7.2). The cells were postfixed for 2 h with 1% osmium tetroxide in the same buffer. The sections were obtained from Ladd LX112 embedded samples and stained with uranyl acetate and lead citrate in the 2168 Carlsberg system (LKB Instruments Inc., Bromma, Sweden). Micrographs were taken with a JEOL JEM-100B operated at 80 kV.

(ii) **Negative staining.** Cooper grids (400 mesh) coated with a thin collodion-carbon supporting film were floated on a droplet of the specimen solution for 25 s, transferred to a droplet of distilled water for 2 s, and then transferred to a droplet of 1% ammonium molybdate stain for 30 s. In the first two steps, excess liquid was removed by shaking the grid, and in the last step, it was removed by blotting the grid with filter paper. The grids were then dried in air. A Philips EM301 microscope was used at an operation voltage of 80 kV, with a 50- μ m objective aperture. Grids were inserted with the specimen side down, i.e., away from the electron source. Tilt series were taken using a eucentric tilt stage with a tilt range of $\pm 60^\circ$. To limit the radiation damage, the focusing was done on the carbon film adjacent to the specimen. Micrographs were recorded at a magnification of 40,000 \times (calibrated against catalase) on Kodak 4489 films and developed in Kodak D19 developer at 20°C for 5 min.

(iii) **Shadowing.** Collodion-carbon coated 600-mesh copper grids were used. As with negative staining, the grids were placed on a droplet of specimen for 25 s and then washed for 2 s. They were then air dried and shadowed with Pd-Pt while rotating at a constant speed in an Edwards evaporator, placed at our disposal at the European Molecular Biology Laboratory, Heidelberg, Federal Republic of Germany.

Computing. The tilt sets of micrographs were checked on an optical diffractometer for control of astigmatism, resolution, and optimum focus. The subsequent analysis was performed under the auspices of Kevin Leonard at the European Molecular Biology Laboratory. The best micrographs, i.e., those with virtually no astigmatism and showing good crystals (good resolution) taken at optimum focus, were scanned on a 25- μ m raster, which corresponds to a real space sampling of 6.25 nm, with an Optronics drum densitometer (System P-1000, Optronics International, Inc., Chelmsford, Mass.). Each scan contains 512 \times 512 points. The scanned area contains ca. 500 unit cells. Computation of Fourier transforms and noise filtering was done as described previously (20).

Three-dimensional reconstruction. The Fourier transform of a one-unit-cell thick crystal, i.e., a two-dimensional crystal, is continuous in the Z^* direction, i.e., perpendicular to the plane of the crystal. According to the projection theorem, the Fourier transform from each tilted image samples a central section in reciprocal space and yields amplitude and phase information for one point for each reflection along the Z^* (14). A common origin in reciprocal space for each image was found using a computer program from R. Henderson and S. Fuller, after first determining phase origin to be exactly on the sixfold axis on the zero tilt by setting the phase values of 0° or 180° , whichever was closest to the observed value after a phase residual minimization procedure. The resulting average phase error for the reflections is 13° . Only reflections

which deviated from one another less than 0.033 nm^{-1} in Z^* , i.e., less than ca. $1/(2 \times \text{crystal thickness})$, were used in the phase-origin refinement and amplitude scaling. The symmetry relations for amplitudes and phases following from the p6 symmetry were employed. The resulting amplitude and phase data points from the combined data set were then sampled by hand from hand-drawn smooth curves at reciprocal intervals of 0.033 nm^{-1} in Z^* . A three-dimensional Fourier synthesis was carried out on a $32 \times 32 \times 32$ matrix.

RESULTS

The S-layer of the *Synechocystis* sp. strain CLII is clearly seen as the outermost surface layer of the ruthenium red-stained, thin-sectioned cell (Fig. 1). The thickness of the S-layer is ca. 14 nm. The space between the S-layer and the outer membrane is ca. 20 nm. This space seems to be filled with thin joining fibers (21).

The isolated fragments of this S-layer show hexagonally arranged subunits, as seen in the negatively stained (ammonium molybdate) material (Fig. 2). In the metal-shadowed sample (Fig. 3), it is seen that each S-layer can consist of several crystalline areas, with slightly varying orientation relative to each other. It is not difficult, however, to find areas large enough for the structural analysis, i.e., containing several hundred unit cells.

The two-dimensional space group is found to be p6 in accordance with the nomenclature of Holser (15). The cell constants are $a = b = 15.2 \text{ nm}$, and $\gamma = 120^\circ$. The ratio $a:b$ is always equal to 1.00 within 1%. A typical diffraction pattern for a nontilted sample is shown in Fig. 4. The resolution is ca. 3 nm.

A filtered projection (Fig. 5) reveals a central hollow cylinder with arms connecting to the neighboring hexamers. The arms are in contact over the crystallographic twofold axes, which means that they are of the delta type by the nomenclature of Stewart and Murray (30).

No density is observed in the region of the threefold axes at this contouring level. This region could, however, contain carbohydrates or any material which is not ordered in the crystalline array.

The present three-dimensional reconstruction is based on seven films, taken with a tilt angle varying between 0 and 49° . Full use of the p6 symmetry was applied in the reconstruction. Amplitude and phase values for the data points on the films were combined to fill the three-dimensional Fourier space. The continuous amplitude and phase lines were then sampled at regular intervals (0.033 nm^{-1}). Examples of two such lines are given (Fig. 6).

A model showing the packing of seven hexamers in the S-layer is shown (Fig. 7). The top and bottom sides of the model are quite differ-

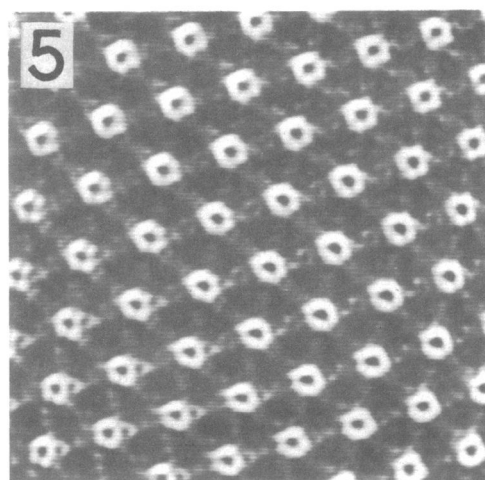
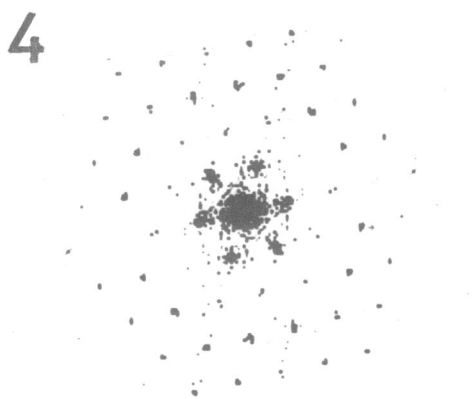
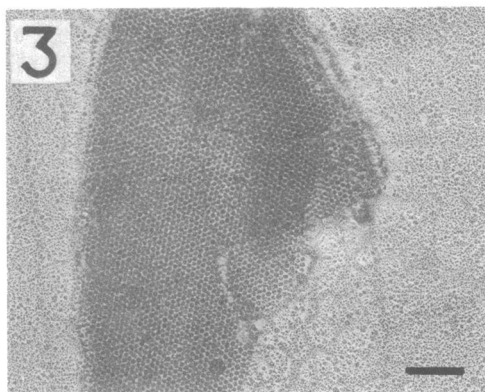
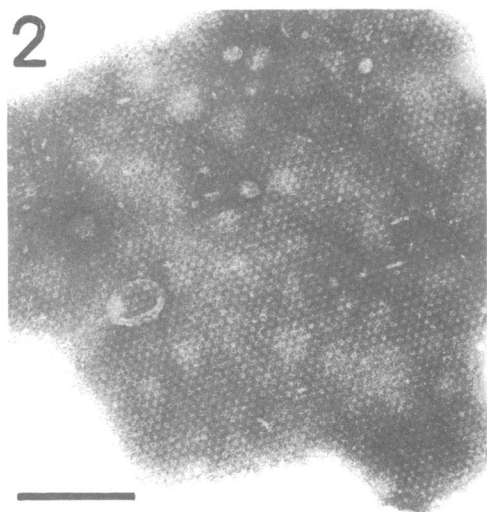
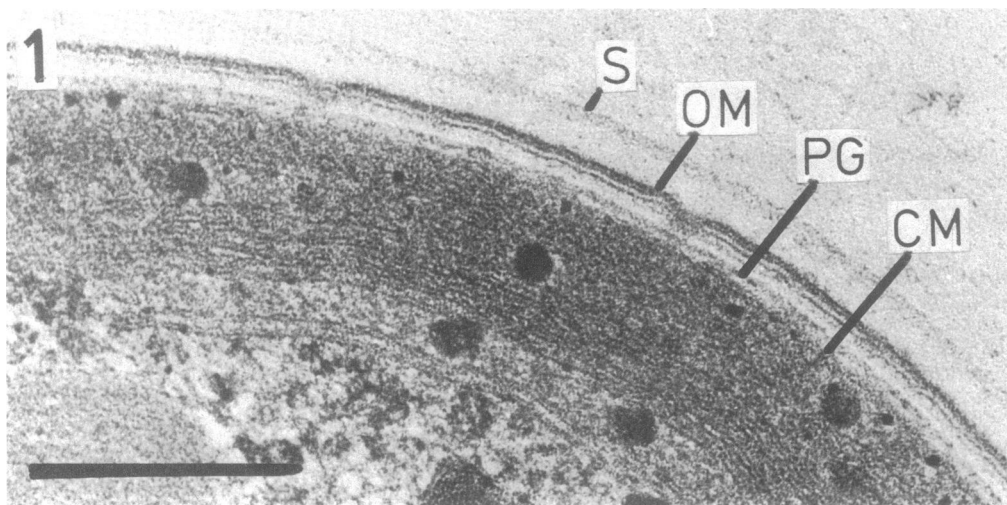


FIG. 1. Cell envelope of the thin-sectioned cell of *Synechocystis* sp. strain CLII. The cytoplasmic membrane (CM), the peptidoglycan layer (PG), the outer membrane (OM), and the S-layer (S) are clearly seen. Scale bar, 0.2 μ m.

FIG. 2. Negatively stained material of the isolated cell envelope fragment with hexagonally arranged subunits. Scale bar, 0.2 μ m.

FIG. 3. Metal-shadowed (Pd-Pt) cell envelope indicating that each S-layer consists of several crystalline areas. Scale bar, 0.2 μ m.

FIG. 4. Diffraction pattern from a negatively stained S-layer. Note the sixfold symmetry of the intensities.

FIG. 5. Filtered projection resulting from the analysis of the diffraction pattern shown in Fig. 4. The center-to-center distance between two neighboring hexamers is 15 nm.

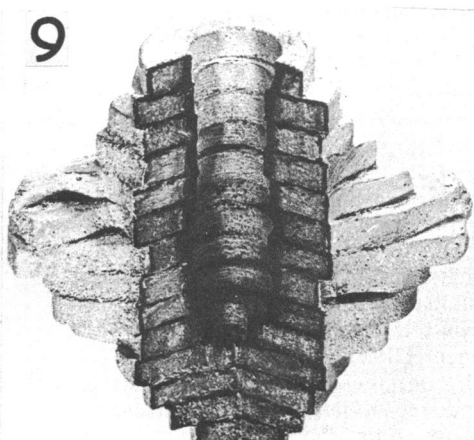
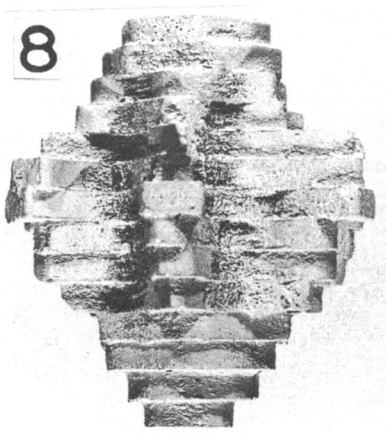
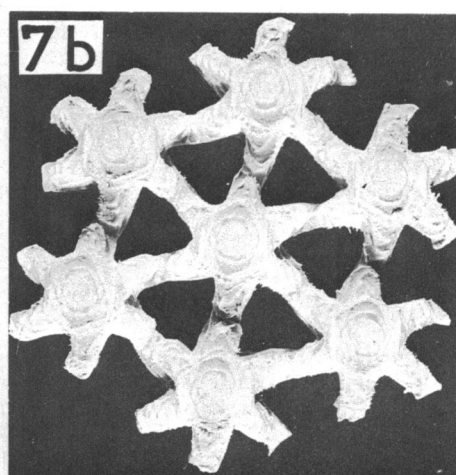
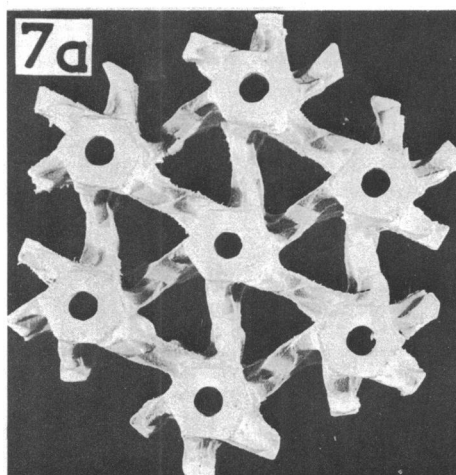
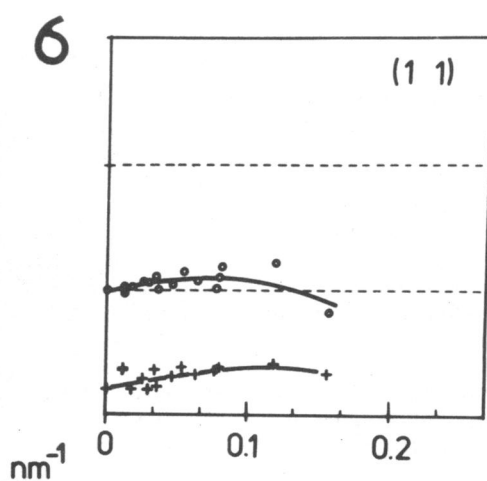
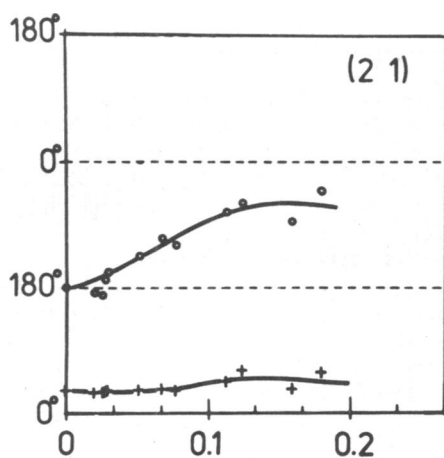


FIG. 6. Sample curves for the variation in amplitudes (+) and phases (o) for two reflections. Z^* is shown along the asxcissa. The amplitudes are given on an arbitrary scale; the units for the phases are given on the ordinate.

FIG. 7. Balsawood model of the S-layer showing (a) the top and (b) bottom sides.

FIG. 8. Side-on view of an isolated hexamer. The arms have been cut at the locations of the twofold axes. The top side is oriented upwards. Each section is ca. 1 nm thick.

FIG. 9. Single hexamer cut open. The cavity is clearly seen to protrude into the protein assembly about 10 nm from the top side. Each section is ca. 1 nm thick.

ent; the bottom side of the main body is closed, whereas there is a cleft on the top. The thickness of the model as it appears in the reconstruction is 14 nm, in good agreement with the value from the thin section (Fig. 1).

A balsawood model of a single hexamer is also shown (Fig. 8). The arms have been cut in the middle between the central cylinders, i.e., over the twofold axes. This cut is not necessarily correct, but at this resolution it is impossible to determine the exact dimensions of the arms. The cavity (central hole) goes 10 nm down from the top end, as is shown in the cut open hexamer (Fig. 9), leaving a closing piece of 4-nm density at the bottom side. The diameter of this cavity measured at the top end is 2.5 nm. The volume of the hexamer is found to be 580 nm³. Assuming a value of 800 daltons per nm³ for the protein, this volume would correspond to about 80% of that calculated from the approximate molecular mass of the monomeric protein (100 kilodaltons), as estimated in sodium dodecyl sulfate-polyacrylamide gel electrophoresis (manuscript in preparation).

DISCUSSION

In the recent report (34) we described the negative staining of single subunits detached from the S-layer of *Synechocystis* sp. strain CLII; they resembled six-pointed stars. That finding is in agreement with the present model, although the dimensions of the detached subunits are larger than what was observed in the crystals. This, however, can be explained by the more severe flattening of the single object compared with the crystal, which is expected.

From negatively stained or metal-shadowed material, or both, it is impossible to determine which side of the molecule is facing the interior of the cell. However, from the sectioned material (Fig. 1), it appears that the end facing the cell is closed and the other end is open. We thus conclude that the top side is open to the exterior of the cyanobacterium. This deduction is also supported by the shape of the molecules in the thin-sectioned cell (Fig. 1).

In conclusion, there seems to be a cavity rather than a hole at the top end. The closed end has been found to face both the supporting film on the grid and to be oriented away from the grid in different experiments. This then indicates that the closed end is real and not a distortion originating from the contact between the S-layer and the supporting foil on the grid.

The protein in the S-layer could be of the glycoprotein type, as is often found in S-layers. We believe that carbohydrates are present and fill the areas around the threefold axes, making

the S-layer a better barrier against the environment. These areas are not, however, visualized in this type of reconstruction as they are probably not well enough ordered. The S-layer seems to be joined to the outer membrane complex by numerous thin fibers (21).

It has been suggested that the function of this layer is to act as a barrier against foreign substances in the environment and also to keep some enzymes within the cell (2, 3, 33). This is a generally accepted hypothesis which still remains to be proved.

ACKNOWLEDGMENTS

The very generous help from Kevin Leonard and co-workers at the European Molecular Biology Laboratory in placing both equipment and expertise at our disposal is gratefully acknowledged. Valuable discussions with the participants in the course "Electron Microscopy and Image Reconstruction" held at the European Molecular Biology Laboratory in April 1982, where this material was partly used, is also appreciated.

B.K. has received financial support from Swedish Natural Science Research Council and T.V. from the Academy of Finland.

LITERATURE CITED

1. Beveridge, T. J. 1979. Surface arrays on wall of *Sporosarcina ureae*. *J. Bacteriol.* **139**:1039-1048.
2. Beveridge, T. J. 1980. Bacterial structure and its implications in the mechanism of infection: a short review. *Can. J. Microbiol.* **26**:643-653.
3. Beveridge, T. J. 1981. Ultrastructure, chemistry, and function of the bacterial wall. *Int. Rev. Cytol.* **72**:229-317.
4. Beveridge, T. J., and R. G. E. Murray. 1974. Superficial macromolecular arrays on the cell wall of *Spirillum putridiconchylum*. *J. Bacteriol.* **119**:1019-1038.
5. Beveridge, T. J., and R. G. E. Murray. 1976. Reassembly *in vitro* of the superficial cell wall components of *Spirillum putridiconchylum*. *J. Ultrastruct. Res.* **55**:105-118.
6. Beveridge, T. J., and R. G. E. Murray. 1976. Dependence of the superficial layers of *Spirillum putridiconchylum* on Ca(2+) or Sr(2+). *Can. J. Microbiol.* **22**:1233-1244.
7. Blaurock, A. E., W. Stoekenius, D. Oesterhelt, and G. L. Scherphof. 1976. Structure of the cell envelope of *Halo-bacterium halobium*. *J. Cell Biol.* **71**:1-22.
8. Buckmire, F. L. A., and R. G. E. Murray. 1970. Studies of the cell wall of *Spirillum serpens*. I. Isolation and partial purification of the outermost cell wall layer. *Can. J. Microbiol.* **16**:1011-1022.
9. Buckmire, F. L. A., and R. G. E. Murray. 1973. Studies of the wall of *Spirillum serpens*. II: Chemical characterization of the outer structural layer. *Can. J. Microbiol.* **19**:59-66.
10. Buckmire, F. L. A., and R. G. E. Murray. 1976. Sub-structure and *in vitro* assembly of the outer, structured layer of *Spirillum serpens*. *J. Bacteriol.* **125**:290-299.
11. Chang, J.-J., K. Leonard, T. Arad, T. Pitt, Y.-X. Zhang, and L.-H. Zhang. 1982. Structural studies of the outer envelope of *Chlamydia trachomatis* by electron microscopy. *J. Mol. Biol.* **161**:579-590.
12. Glaeser, R. H., W. Chiu, and D. Grano. 1979. Structure of surface layer protein of the outer membrane of *Spirillum serpens*. *J. Ultrastruct. Res.* **66**:236-242.
13. Hastie, A. T., and C. C. Brinton, Jr. 1979. Isolation, characterization, and *in vitro* assembly of the tetragonally arrayed layer of *Bacillus sphaericus*. *J. Bacteriol.* **138**:999-1009.
14. Henderson, R., and P. N. T. Unwin. 1975. Three-dimen-

- sional model of purple membrane obtained by electron microscopy. *Nature* (London) **257**:28–32.
15. Holser, W. T. 1958. Point groups and plane groups in a two-sided plane and their subgroups. *Kristallgeom. Kristallphys. Kristallchem. Z. Kristallogr.* **110**:266–281.
 16. Kay, W. W., J. T. Buckley, E. E. Ishiguro, B. M. Phipps, J. P. L. Monette, and T. J. Trust. 1981. Purification and disposition of a surface protein associated with virulence of *Aeromonas salmonicida*. *J. Bacteriol.* **147**:1077–1084.
 17. Kessel, M. 1978. A unique crystalline wall layer in the cyanobacterium *Microcystis marginata*. *J. Ultrastruct. Res.* **62**:203–212.
 18. Koval, S. F., and R. G. E. Murray. 1981. Cell wall proteins of *Aquaspirillum serpens*. *J. Bacteriol.* **146**:1083–1090.
 19. Kubler, O., A. Engel, H. P. Zingsheim, B. Emde, M. Hahn, W. Heisse, and W. Baumeister. 1980. Structure of the HPI-layer of *Micrococcus radiodurans*, p. 11–21. In W. Baumeister and W. Vogell (ed.) *Electron microscopy at molecular dimensions*. Springer-Verlag, Berlin.
 20. Leonard, K., P. Wingfield, T. Arad, and H. Weiss. 1981. Three-dimensional structure of Ubiquinol: cytochrome c reductase from *Neurospora* mitochondria determined by electron microscopy of membrane crystals. *J. Mol. Biol.* **149**:259–274.
 21. Lounatmaa, K., T. Vaara, K. Österlund, and M. Vaara. 1980. Ultrastructure of the cell wall of a *Synechocystis* strain. *Can. J. Microbiol.* **26**:204–208.
 22. Luft, J. H. 1971. Ruthenium red and violet. I. Chemistry, purification, methods for use for electron microscopy and mechanism of action. *Anat. Rec.* **171**:347–368.
 23. Saxton, W. O., and W. Baumeister. 1982. The correlation averaging of a regularly arranged bacterial cell envelope protein. *J. Microsc. (Oxford)* **127**:127–138.
 24. Sleytr, U. B. 1978. Regular arrays of macromolecules on bacterial cell walls: structure, chemistry, assembly and function. *Int. Rev. Cytol.* **53**:1–64.
 25. Sleytr, U. B., P. Messner, P. Schiske, and D. Pum. 1982. Periodic surface structures on procaryotic cells. *Proc. 10th Int. Congr. Electron Microsc., Hamburg.* **3**:1–8.
 26. Smit, J., D. A. Grano, R. M. Glaeser, and N. Agabian. 1981. Periodic surface array in *Caulobacter crescentus*: fine structure and chemical analysis. *J. Bacteriol.* **146**:1135–1150.
 27. Stanier, R. Y., R. Kunisawa, M. Mandel, and G. Cohen-Bazire. 1971. Purification and properties of unicellular blue-green algae (order *Croococcales*). *Bacteriol. Rev.* **35**:171–205.
 28. Stanier, R. Y., and G. Cohen-Bazire. 1977. Phototropic procaryotes: the cyanobacteria. *Annu. Rev. Microbiol.* **31**:225–274.
 29. Stewart, M., and T. J. Beveridge. 1980. Structure of the regular surface layer of *Sporosarcina ureae*. *J. Bacteriol.* **142**:302–309.
 30. Stewart, M., and R. G. E. Murray. 1982. Structure of the regular surface layer of *Aquaspirillum serpens* MW5. *J. Bacteriol.* **150**:348–357.
 31. Stewart, M. T., T. J. Beveridge, and R. G. E. Murray. 1980. Structure of the regular surface layer of *Spirillum putridiconchylum*. *J. Mol. Biol.* **137**:1–8.
 32. Taylor, K. A., J. F. Deatherage, and L. A. Amos. 1982. Structure of the S-layer of *Sulfolobus acidocaldarius*. *Nature* (London) **299**:840–842.
 33. Trust, T. J., P. S. Howard, J. B. Chamberlain, E. E. Ishiguro, and J. T. Buckley. 1980. Additional surface protein in autoaggregating strains of atypical *Aeromonas salmonicida*. *FEMS Microbiol. Lett.* **9**:35–38.
 34. Vaara, T. 1982. The outermost surface structures in chroococcacean cyanobacteria. *Can. J. Microbiol.* **28**:929–941.
 35. Vaara, T., and Lounatmaa, K. 1980. Freeze-fracturing of the cell envelope of the *Synechocystis* CB3. *FEMS Microbiol. Lett.* **9**:203–209.
 36. Vaara, T., M. Vaara, and S. Niemelä. 1979. Two improved methods for obtaining axenic cultures of cyanobacteria. *Appl. Environ. Microbiol.* **38**:1011–1014.
 37. Weiss, R. L. 1974. Subunit cell wall of *Sulfolobus acidocaldarius*. *J. Bacteriol.* **118**:275–284.